

Luminescence and structure of Eu^{2+} -doped $\text{Ba}_2\text{CaMg}_2\text{Si}_6\text{O}_{17}$

Beiling Yuan^a, Yanlin Huang^a, Young Moon Yu^b, Hyo Jin Seo^{c,*}

^a College of Chemistry, Chemical Engineering and Materials Science, Soochow University, Suzhou 215123, China

^b LED-Marin Convergence Technology R&BD Center, Pukyong National University, Busan 608-739, Republic of Korea

^c Department of Physics, Pukyong National University, Busan 608-737, Republic of Korea

Received 23 September 2011; received in revised form 24 October 2011; accepted 26 October 2011

Available online 3 November 2011

Abstract

Eu^{2+} -activated $\text{Ba}_2\text{CaMg}_2\text{Si}_6\text{O}_{17}$ phosphors were synthesized by conventional solid-state reaction. The phase formation was confirmed by X-ray powder diffraction measurement. The photoluminescence excitation and emission spectra were investigated. The phosphor presents blue-emitting luminescence. The crystallographic sites of Eu^{2+} ions in $\text{Ba}_2\text{CaMg}_2\text{Si}_6\text{O}_{17}$ host were discussed on the base of luminescence properties and the crystal structure. The lightly Eu^{2+} -doped sample shows one luminescence center for the Eu^{2+} ions on Ba^{2+} sites, while there are two luminescence centers for the Eu^{2+} ions on both the Ba and Ca sites in heavily Eu^{2+} -doped sample. The dependence of luminescence intensity on temperatures and the activation energy (ΔE) for the thermal quenching were reported. The phosphor shows an excellent thermal stability on temperature quenching because of the special layered structure of Ba^{2+} ions in the interlayer between SiO_4 layers.

© 2011 Elsevier Ltd and Techna Group S.r.l. All rights reserved.

Keywords: Luminescence; Eu^{2+} ; Optical materials and properties; Silicate

1. Introduction

The luminescence properties, structures and applications of Eu^{2+} -doped solids have been intensively investigated during the past decade [1,2]. Eu^{2+} -doped phosphors with various crystal structures have been paid great attentions due to the applications in white light-emitting diodes (W-LEDs) [3,4], long lasting luminescent phosphors [5], and PDP display under VUV excitation [6].

In recent years, Eu^{2+} -doped phosphors have been widely investigated as phosphors in solid-state lighting. Usually, Eu^{2+} -doped phosphors with the strong covalent bond, weak electron–phonon coupling strength and distorted coordination exhibit broad excitation band and excellent thermal stability. Such kinds of phosphors, for example, Eu^{2+} -doped silicon-based oxynitrides and nitrides [7], $(\text{Sr},\text{Ba},\text{Ca})\text{Si}_2\text{N}_2\text{O}_2$ [8–10], CaAlSiN_3 [11], $\text{LaSi}_3\text{N}_5:\text{Eu}^{2+}$ [12], have been demonstrated to be excellent for W-LEDs application. However, the very high firing temperatures and high nitrogen pressures are required for their synthesis, resulting in higher production cost.

Silicates have strong and rigid characteristics of partly covalent Si–O bond. The rigid frameworks of silicate lattices can provide the distorted coordination around the emission ion [13]. Compared with aluminates and sulphides, Eu^{2+} -doped silicates have some advantages, such as a chemical and physical stability, a varied luminescence, and excellent water-resistance. In recent years, Eu^{2+} -doped silicates have attracted further attentions for the significant applications in W-LEDs because the phosphors can absorb ultraviolet or blue light from LED chips and efficiently emit visible light [14–16].

Among Eu^{2+} -doped silicates, many studies on the luminescence properties of Eu^{2+} -activated alkaline earth magnesium silicates have been reported, e.g., $\text{M}_2\text{MgSi}_2\text{O}_7:\text{Eu}^{2+}$ ($\text{M} = \text{Ca}, \text{Sr}, \text{Ba}$) [6,17,18], $\text{BaMg}_2\text{Si}_2\text{O}_7:\text{Eu}^{2+}$, Mn^{2+} [5], $\text{Sr}_2\text{MgSi}_2\text{O}_7:\text{Eu}^{2+}$, Dy^{3+} [19], $\text{M}_3\text{MgSi}_2\text{O}_8:\text{Eu}^{2+}$ ($\text{M} = \text{Ca}, \text{Sr}, \text{Ba}$) [20], $\text{BaCa}_2\text{MgSi}_2\text{O}_8:\text{Eu}^{2+}$ [21], MgSiO_3 -based glass–ceramics [22], MMgSiO_4 ($\text{M} = \text{Ca}, \text{Sr}$ and Ba) and MMgSi_2O_8 ($\text{M} = \text{Ca}, \text{Sr}$ and Ba) [17]. Alkaline earth magnesium silicates can emit rich luminescence due to the various crystal fields, and show high thermal stabilities.

In this work Eu^{2+} -doped $\text{Ba}_2\text{CaMg}_2\text{Si}_6\text{O}_{17}$ phosphors were synthesized. The structure was investigated by powder X-ray diffraction (XRD) measurement. The photoluminescence excitation and emission spectra were measured. The

* Corresponding author.

E-mail address: hjseo@pknu.ac.kr (H.J. Seo).

luminescence and structural occupancy of Eu^{2+} ions in the host lattices were discussed.

2. Experimental details

The preparation of $\text{Ba}_2\text{CaMg}_2\text{Si}_6\text{O}_{17}:\text{Eu}^{2+}$ was carried out by solid state reaction method. The raw materials were high-purity BaCO_3 , CaCO_3 , $4(\text{MgCO}_3)\cdot\text{Mg}(\text{OH})_2\cdot 5\text{H}_2\text{O}$ (magnesium carbonate basic pentahydrate), SiO_2 and Eu_2O_3 . The stoichiometric amounts of starting materials were thoroughly ground in an agate mortar. The mixture was firstly heated at 1000°C for 6 h in air. Then the fired samples were heated at 1200°C for 10 h in a reductive atmosphere (active carbon).

The XRD pattern was collected on a Rigaku D/Max-2000 diffractometer operating at 40 kV, 30 mA with Bragg–Brentano geometry by using $\text{Cu K}\alpha$ radiation ($\lambda = 1.5418 \text{ \AA}$). The optical excitation and emission spectra were recorded by a Perkin-Elmer LS-50B luminescence spectrometer and a Hitachi F-4500 fluorescence spectrophotometer. To study thermal quenching of the luminescence, the same spectrometer was equipped with a homemade heating cell.

3. Results and discussion

3.1. The phase formation and crystal structure

Fig. 1 shows the X-ray powder diffraction patterns of 1.0 and 10.0 mol% Eu^{2+} -doped $\text{Ba}_2\text{CaMg}_2\text{Si}_6\text{O}_{17}$ compared with the PDF2 Card Number 15-0799 ($\text{Ba}_2\text{CaMg}_2\text{Si}_6\text{O}_{17}$) selected from the International Centre for Diffraction Data (ICDD) database. By a comparison between them, the positions and relative intensities of the main peaks in the samples well match the standard card. No impurity lines were observed, and all the reflections could be well indexed to a $\text{Ba}_2\text{CaMg}_2\text{Si}_6\text{O}_{17}$ single phase.

$\text{Ba}_2\text{CaMg}_2\text{Si}_6\text{O}_{17}$ is isostructural with pellyite: $\text{Ba}_2\text{Ca}(\text{Fe},\text{Mg})_2\text{Si}_6\text{O}_{17}$, and crystallizes in the orthorhombic structure in the space group $Cmcm$ (63) with the lattice parameters

$a = 15.759 \text{ \AA}$, $b = 7.115 \text{ \AA}$, $c = 14.130 \text{ \AA}$, $Z = 4$, and $\alpha = \beta = \gamma = 90^\circ$ [23]. Fig. 2 illustrates the schematic views of $\text{Ba}_2\text{CaMg}_2\text{Si}_6\text{O}_{17}$ structure along b -direction and the comparison of the coordination geometries around the Ca and Ba. The framework is built with layered structure with the strings arranged in the sequence of $-\text{CaO}_6-\text{MgO}_4-\text{MgO}_4-\text{CaO}_6-$, $-\text{SiO}_4-$, $-\text{BaO}_{10}-$, $-\text{SiO}_4-$ along a axis. In this structure $[\text{CaO}_6]$ octahedra and double $[\text{MgO}_4]$ tetrahedra are located in a layer. The bond distances of Ca–O range from 2.321 to 2.4092 \AA . The corner-shared SiO_4 tetrahedra form zig-zag chains. The $-\text{BaO}_{10}-$ layer is in interlayer between two $[\text{SiO}_4]$ layers. Ba^{2+} ions on Wyckoff 8 g positions are coordinated by ten neighboring oxygen ions of each layer of $[\text{SiO}_4]$ tetrahedra and $[\text{CaO}_6]$ octahedra. The bond distances of Ba–O range from 2.560 to 3.2413 \AA . The whole framework forms two dimensional sheets structure.

3.2. The excitation and emission spectra

Fig. 3 shows the typical luminescence spectra of $\text{Ba}_2\text{CaMg}_2\text{Si}_6\text{O}_{17}:x\text{Eu}^{2+}$ ($x = 0.01, 0.1$). The excitation spectra of $\text{Ba}_2\text{CaMg}_2\text{Si}_6\text{O}_{17}:\text{Eu}^{2+}$ consist of broad absorption bands from 250 to 450 nm attributed to $4f-5d$ transition of Eu^{2+} ions. This indicates that the phosphor can well match with the light of UV-LED chips (360–400 nm), which is essential for improving the efficiency of W-LEDs.

The emission spectra of $\text{Ba}_2\text{CaMg}_2\text{Si}_6\text{O}_{17}:\text{Eu}^{2+}$ shows bright blue luminescence with the maximum wavelength at 455–466 nm from the $4f^65d \rightarrow 4f^7$ ($^8\text{S}_{7/2}$) transitions in Eu^{2+} ions. The dependence of the experimental luminescence intensity on the Eu^{2+} doping concentrations is shown in inset in Fig. 3(a). The luminescence intensity increases with increasing the Eu^{2+} -doping until a maximum intensity about $x = 0.1$ (10.0 mol%) is reached, and then it decreases because of conventional concentration quenching process.

The luminescence maximum positions of $\text{Ba}_2\text{CaMg}_2\text{Si}_6\text{O}_{17}:x\text{Eu}^{2+}$ samples are listed in Table 1. It can be found that the luminescence positions of Eu^{2+} ions show the dependence on the doping levels of Eu^{2+} . The emission spectra of $\text{Ba}_2\text{CaMg}_2\text{Si}_6\text{O}_{17}:\text{Eu}^{2+}$ in Fig. 3, especially the spectrum for $\text{Ba}_2\text{CaMg}_2\text{Si}_6\text{O}_{17}:\text{Eu}^{2+}$ 10 mol% (Fig. 3 b), show the asymmetric shapes, indicating only one Eu^{2+} luminescence center in the host. The spectra could be reproduced as a superposition of at least two Gaussian components. The suggested two emission components for $\text{Ba}_2\text{CaMg}_2\text{Si}_6\text{O}_{17}:\text{Eu}^{2+}$ 1.0 mol%, i.e., 545 nm and 505 nm, are shown in Fig. 3(a). And Fig. 3(b) is the representative Gaussian fitting into two components peaked at 466 nm and 545 nm for $\text{Ba}_2\text{CaMg}_2\text{Si}_6\text{O}_{17}:\text{Eu}^{2+}$ 10 mol%.

In the structure of $\text{Ba}_2\text{CaMg}_2\text{Si}_6\text{O}_{17}$, there are two non-equivalent sites Ca and Ba as shown in Fig. 2(b). Ca^{2+} ions occupy the $4a$ site surrounded by six oxygen atoms with $2/m$ symmetry. The Ba^{2+} ions in the 8 g site are surrounded by ten oxygen atoms with m symmetry [23]. The ionic radii of Eu^{2+} ion is $r = 1.35 \text{ \AA}$ (coordination number CN = 10). The Ba^{2+} ions have bigger radii of $r = 1.52 \text{ \AA}$ (CN = 10) [24]. When Eu^{2+} is incorporated into $\text{Ba}_2\text{CaMg}_2\text{Si}_6\text{O}_{17}$ host, it would prefer to substitute one Ba^{2+} site. However, Eu^{2+} ion with CN = 6 has a

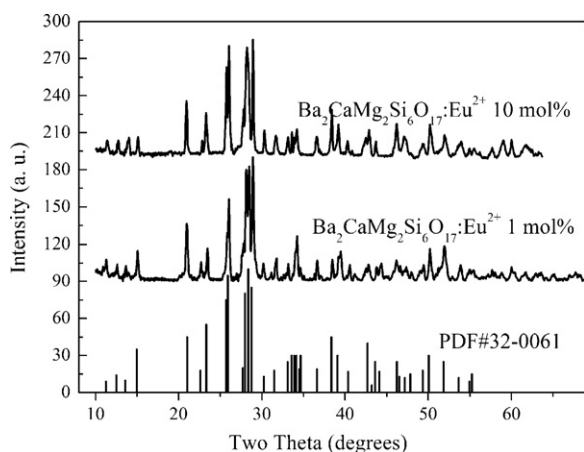


Fig. 1. XRD patterns Eu^{2+} -doped $\text{Ba}_2\text{CaMg}_2\text{Si}_6\text{O}_{17}$ compared with the corresponding PDF2 Card Number 32-0061.

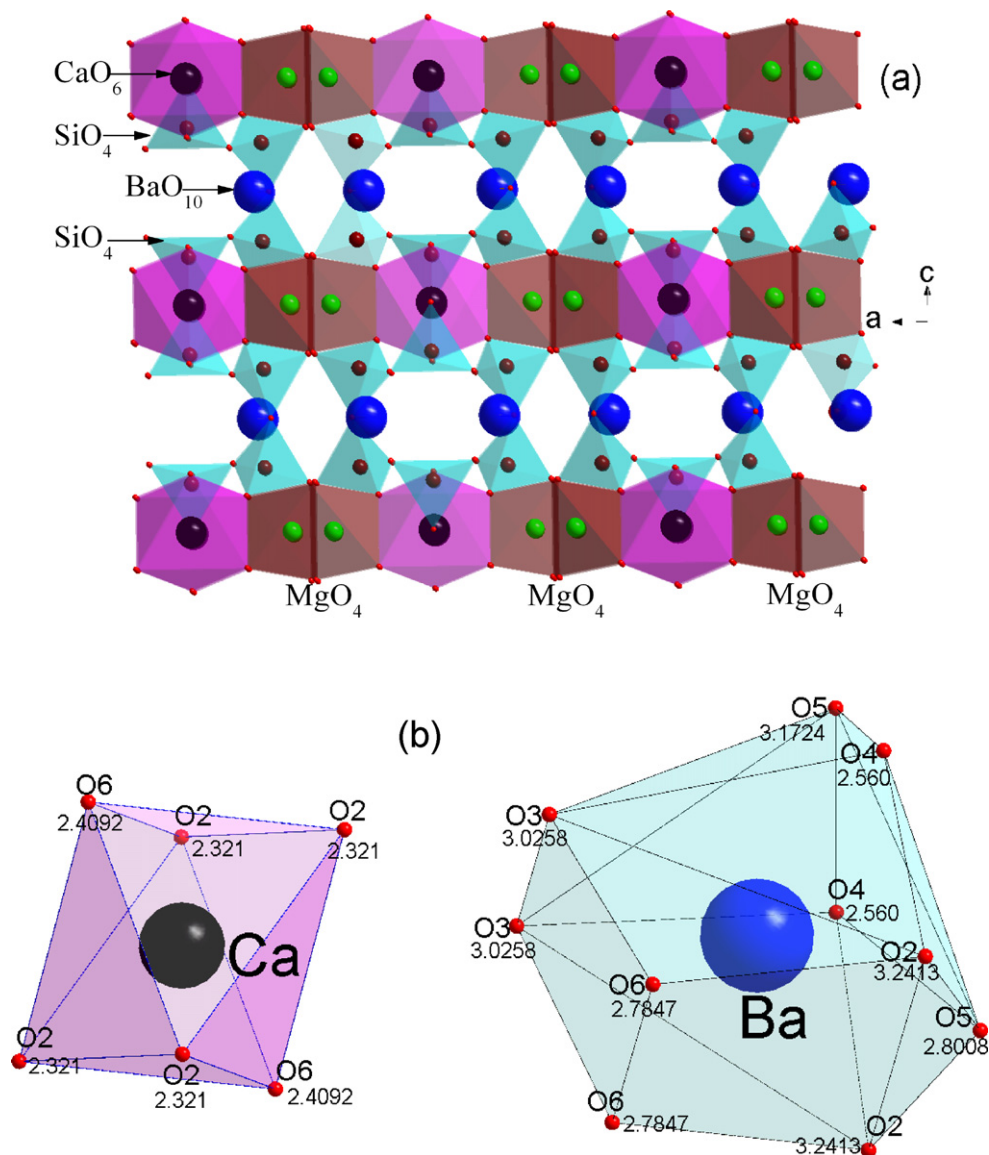


Fig. 2. (a) The schematic views of $\text{Ba}_2\text{CaMg}_2\text{Si}_6\text{O}_{17}$ structure along b -direction; (b) the comparison of the coordination geometries around the Ca and Ba.

radius of $r = 1.17 \text{ \AA}$, which is comparable to that of Ca^{2+} ions 1.0 \AA (CN = 6). So it is reasonable for another substitution of Eu^{2+} for Ca^{2+} ions if the doping level is high, e.g., 10 mol%.

In the structure of $\text{Ba}_2\text{CaMg}_2\text{Si}_6\text{O}_{17}$ the bond-length of $\text{Ca}^{2+}\text{-O}$ is shorter than that of $\text{Ba}^{2+}\text{-O}$. Thus, the high-energy emission at 466 nm should originate from the Eu^{2+} ions, which occupy the loose crystal circumstance with larger Ba-O bond length (Ba site); and the low-energy emission at 545 nm can be ascribed to the Eu^{2+} ions occupying the compact crystal circumstance with shorter $\text{Ca}^{2+}\text{-O}$ bond length (Ca site).

Table 1

The luminescence maximum positions and decay lifetimes of $\text{Ba}_2\text{CaMg}_2\text{Si}_6\text{O}_{17}:x\text{Eu}^{2+}$ samples.

x	0.01	0.03	0.05	0.07	0.1	0.12	0.15
Position (nm)	455	455	458	462	466	468	470
τ (μs)	0.61	0.58	0.55	0.53	0.5	0.45	0.35

Usually, the crystal field should become stronger with increasing Eu^{2+} doping (on Ba site) because the ionic radius of Eu^{2+} is smaller than Ba^{2+} . It is a common phenomenon that the luminescence spectra should have an obvious blue-shift along with the increasing doping of Eu^{2+} for Ba^{2+} -substitution [6]. However, the luminescence of $\text{Ba}_2\text{CaMg}_2\text{Si}_6\text{O}_{17}:\text{Eu}^{2+}$ shifts to the longer wavelength with the increase of Eu^{2+} concentration as shown in Table 1. Therefore, the wavelength shift in Table 1 can also be the results of the replace of Eu^{2+} ions on the Ca^{2+} sites.

3.3. The luminescence decay and lifetimes

The reprehensive decay curves of 1.0 mol% and 10 mol% Eu^{2+} -doped $\text{Ba}_2\text{CaMg}_2\text{Si}_6\text{O}_{17}$ are shown in Figs. 4 and 5, respectively. The fitted luminescence lifetimes are listed in Table 1. The luminescence decay curve of $\text{Ba}_2\text{CaMg}_2\text{Si}_6\text{O}_{17}:\text{Eu}^{2+}$ 1.0 mol% is nearly single-exponential, which

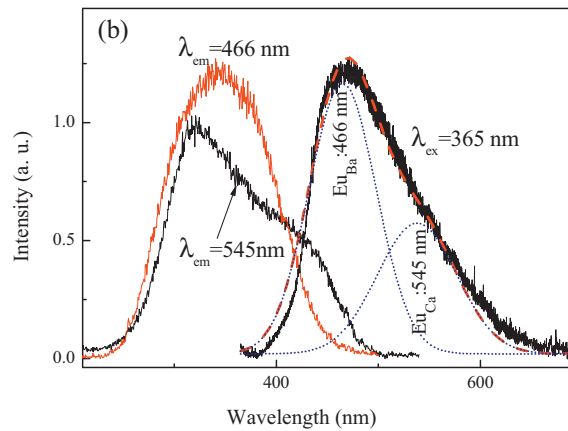
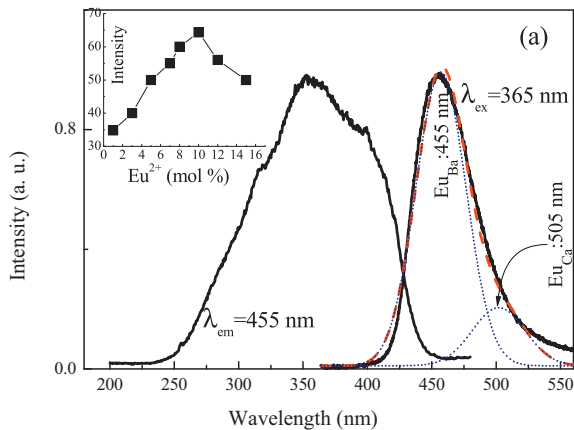


Fig. 3. The excitation and emission spectra of 1.0 mol% (a) and 10 mol% Eu^{2+} -doped $\text{Ba}_2\text{CaMg}_2\text{Si}_6\text{O}_{17}$. Inset in (a) is the doping concentration dependent luminescence intensities of $\text{Ba}_2\text{CaMg}_2\text{Si}_6\text{O}_{17}:\text{Eu}^{2+}$ on the doping levels (mol%).

can be fitted in an exponential equation with a lifetime of $0.61 \mu\text{s}$ (Fig. 4). In $\text{Ba}_2\text{CaMg}_2\text{Si}_6\text{O}_{17}:\text{Eu}^{2+}$ 10 mol% the decay time of shorter wavelength emission band at 466 nm is fitted to be $0.5 \mu\text{s}$ (Fig. 5). The longer emission at 545 nm has a longer lifetime of $0.91 \mu\text{s}$. The noticeable difference of decay times and the different excitation spectra (in Fig. 3(b)) testify the different Eu^{2+} luminescence centers in $\text{Ba}_2\text{CaMg}_2\text{Si}_6\text{O}_{17}$.

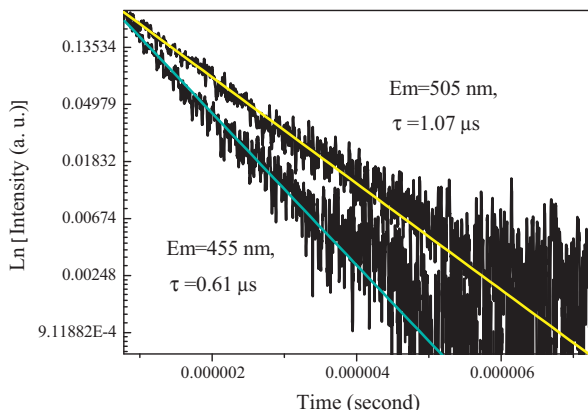


Fig. 4. The luminescence decay curve of $\text{Ba}_2\text{CaMg}_2\text{Si}_6\text{O}_{17}:\text{Eu}^{2+}$ 1.0 mol%.

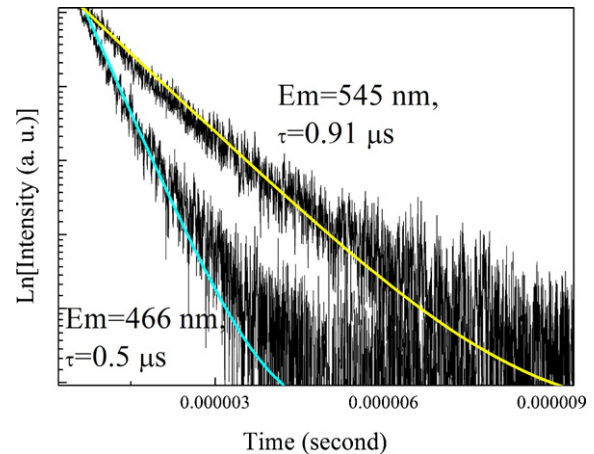


Fig. 5. The decay curves of emission bands at 466 nm and 545 nm in $\text{Ba}_2\text{CaMg}_2\text{Si}_6\text{O}_{17}:\text{Eu}^{2+}$ 10 mol% under the excitation of 355 nm at 297 K.

3.4. The thermal stability of luminescence

Fig. 6 shows the temperature dependence of luminescence intensity of $\text{Ba}_2\text{CaMg}_2\text{Si}_6\text{O}_{17}:\text{Eu}^{2+}$ 10 mol%. At 150°C , the emission intensity of $\text{Ba}_2\text{CaMg}_2\text{Si}_6\text{O}_{17}:\text{Eu}^{2+}$ 10 mol% decrease about 10% of the initial value, indicating a weak thermal quenching behavior. The activation energy (ΔE) for the thermal quenching of the Eu^{2+} emission was determined by a modified Arrhenius equation as follows [25]:

$$I_T = \frac{I_0}{1 + c \exp(-\Delta E/kT)} \quad (1)$$

where I_0 is the initial emission intensity, I_T is the intensity at different temperatures, ΔE is the activation energy of thermal quenching, c is a constant for a certain host, and k is the Boltzmann constant ($8.617 \times 10^{-5} \text{ eV K}^{-1}$). Inset in Fig. 6 plots of $\ln[(I_0/I_T) - 1]$ vs. $1000/T$, which is linear with a slope of -2.56 . According to Eq. (1), the activation energy ΔE was calculated to be 0.22 eV .

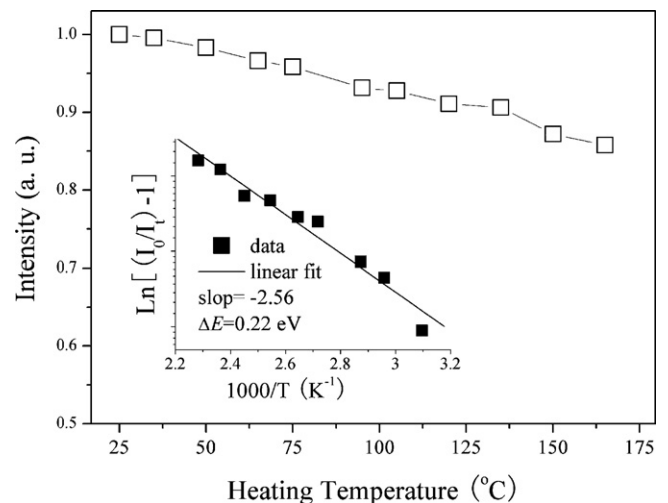


Fig. 6. The integrated emission intensity normalized with respect to the value at 25°C ; inset: the activation energies of the thermal quenching fitted in Eq. (1).

The results show that $\text{Ba}_2\text{CaMg}_2\text{Si}_6\text{O}_{17}:\text{Eu}^{2+}$ has efficient luminescence and good thermal stability. This is due to its characteristics of crystal structure. As shown in Fig. 2(a), $\text{Ba}_2\text{CaMg}_2\text{Si}_6\text{O}_{17}$ has typical layered structure with the Ba^{2+} ion layer between distorted layers of $[\text{SiO}_4]$ tetrahedra.

Usually the Eu^{2+} -activated alkaline earth magnesium silicates, especially the ones with layered structure, could show efficient luminescence and high stability due to the Si–O high covalent bonding, for example, $\text{Ba}_2\text{MgSi}_2\text{O}_7:\text{Eu}^{2+}$ with a two-dimensional structure. For such kinds of alkaline earth magnesium silicates with layered structure, Komeno et al. [6] have suggested that the critical concentration of emission intensity is very high because of the low probability for the excitation energy to be trapped by killer centers in the low dimension of a host. And this kind of compounds has a high thermal quenching temperature because of low thermal vibration by the barium ion's heavy atomic weight.

4. Conclusions

The blue-emitting phosphors of $\text{Ba}_2\text{CaMg}_2\text{Si}_6\text{O}_{17}:\text{Eu}^{2+}$ were synthesized, and its luminescence properties were investigated. The phosphor can be efficiently excited by visible lights (350–450 nm), yielding the intense blue emission at 455–466 nm, which is depended on the Eu^{2+} doping levels. The lightly Eu^{2+} -doped sample, e.g., $\text{Ba}_2\text{CaMg}_2\text{Si}_6\text{O}_{17}:\text{Eu}^{2+}$ 1.0 mol%, shows one dominated emission band from the substituted Ba^{2+} site and a minor band from the Eu^{2+} ions on Ca^{2+} sites. The heavily Eu^{2+} -doped sample $\text{Ba}_2\text{CaMg}_2\text{Si}_6\text{O}_{17}:\text{Eu}^{2+}$ 10 mol% display characteristic two emission components with high energy emission band at 466 nm from Eu^{2+} at Ba^{2+} site and the other one 545 nm from Ca^{2+} site. At 150 °C, the decrease in emission intensity is 10% of the initial value. The luminescence of $\text{Ba}_2\text{CaMg}_2\text{Si}_6\text{O}_{17}:\text{Eu}^{2+}$ possess higher thermal stability, which are related to the special layered crystal structure.

Acknowledgments

This work was financially supported by the Pukyong National University Research Fund in 2011 (PK-2011-29).

References

- [1] P. Dorenbos, Energy of the first $4f^7 \rightarrow 4f^65d$ transition of Eu^{2+} in inorganic compounds, *J. Lumin.* 104 (2003) 239–260.
- [2] P. Dorenbos, Energy of the $\text{Eu}^{2+} 5d$ state relative to the conduction band in compounds, *J. Lumin.* 128 (2008) 578–582.
- [3] C.C. Lin, R.S. Liu, Advances in phosphors for light-emitting diodes, *J. Phys. Chem. Lett.* 2 (2011) 1268–1277.
- [4] L. Chen, C.C. Lin, C.W. Yeh, R.S. Liu, Rare-earth activated nitride phosphors: synthesis, luminescence and applications, *Materials* 3 (2010) 2172–2195.
- [5] S. Abe, K. Uematsu, K. Toda, M. Sato, Luminescent properties of red long persistence phosphors, $\text{BaMg}_2\text{Si}_2\text{O}_7:\text{Eu}^{2+}$, Mn^{2+} , *J. Alloys Compd.* 408–412 (2006) 911–914.
- [6] A. Komeno, K. Uematsu, K. Toda, M. Sato, VUV properties of Eu-doped alkaline earth magnesium silicate, *J. Alloys Compd.* 408–412 (2006) 871–874.
- [7] R.J. Xie, N. Hirotsuki, Silicon-based oxynitride and nitride phosphors for white LEDs—a review, *Sci. Technol. Adv. Mater.* 8 (2007) 588–600.
- [8] B.Y. Han, K.S. Sohn, Ternary combinatorial library of $(\text{Sr},\text{Ba},\text{Ca})\text{Si}_2\text{N}_2\text{O}_2$ phosphors in terms of photoluminescence and color chromaticity, *Electrochem. Solid-State Lett.* 13 (2010) J62–J64.
- [9] Y.C. Fang, P.C. Kao, Y.C. Yang, S.Y. Chua, Two-step synthesis of $\text{SrSi}_2\text{O}_2\text{N}_2:\text{Eu}^{2+}$ green oxynitride phosphor: electron–phonon coupling and thermal quenching behavior, *J. Electrochem. Soc.* 158 (2011) J246–J249.
- [10] V. Bachmann, T. Justel, A. Meijerink, C. Ronda, P.J. Schmidt, Luminescence properties of $\text{SrSi}_2\text{O}_2\text{N}_2$ doped with divalent rare earth ions, *J. Lumin.* 121 (2006) 441–449.
- [11] K. Uheda, N. Hirotsuki, Y. Yamamoto, A. Naito, T. Nakajima, H. Yamamoto, Luminescence properties of a red phosphor, $\text{CaAlSiN}_3:\text{Eu}^{2+}$, for white light-emitting diodes, *Electrochem. Solid-State Lett.* 9 (2006) H22–H25.
- [12] Y. Zhou, Y. Yoshizawa, K. Hirao, Z. Lenčič, P. Šajgalík, Combustion synthesis of $\text{LaSi}_3\text{N}_5:\text{Eu}^{2+}$ phosphor powders, *J. Eur. Ceram. Soc.* 31 (2011) 151–157.
- [13] K. Toda, Y. Kawakami, S. Kousaka, Y. Ito, A. Komeno, K. Uematsu, M. Sato, New silicate phosphors for a white LED, *IEICE Trans. Electron.* E89-C (2006) 1406–1412.
- [14] S.H. Lee, H.Y. Koo, Y.C. Kang, Characteristics of α' - and β - $\text{Sr}_2\text{SiO}_4:\text{Eu}^{2+}$ phosphor powders prepared by spray pyrolysis, *Ceram. Int.* 36 (2010) 1233–1238.
- [15] S.H. Lee, H.Y. Koo, S.Y. Lee, M.J. Lee, Y.C. Kang, Effect of BaF_2 as the source of Ba component and flux material in the preparation of $\text{Ba}_{1-x}\text{Sr}_{0.88-x}\text{SiO}_4:\text{Eu}_{0.02}$ phosphor by spray pyrolysis, *Ceram. Int.* 36 (2010) 339–343.
- [16] Z. Shi, W. Yang, S. Bai, G. Qiao, Z. Jin, Preparation of Eu^{2+} -doped AlN phosphors by plasma activated sintering, *Ceram. Int.* 37 (2011) 2051–2054.
- [17] S.H.M. Poort, H.M. Reijnhoudt, H.O.T. van der Kuip, G. Blasse, Luminescence of Eu^{2+} in silicate host lattices with alkaline earth ions in a row, *J. Alloys Compd.* 241 (1996) 75–81.
- [18] J.M. Kim, S.J. Park, K.H. Kim, H.W. Choi, The luminescence properties of $\text{M}_2\text{MgSi}_2\text{O}_7:\text{Eu}^{2+}$ ($\text{M} = \text{Sr}, \text{Ba}$) nano phosphor in ultraviolet light emitting diodes, *Ceram. Int.*, in press, doi:10.1016/j.ceramint.2011.05.100.
- [19] Y. Xu, D. Chen, Combustion synthesis and photoluminescence of $\text{Sr}_2\text{MgSi}_2\text{O}_7:\text{Eu},\text{Dy}$ long lasting phosphor nanoparticles, *Ceram. Int.* 34 (2008) 2117–2120.
- [20] J.S. Kim, Y.H. Park, J.C. Choi, H.L. Park, Temperature-dependent emission spectrum of $\text{Ba}_3\text{MgSi}_2\text{O}_8:\text{Eu}^{2+}$, Mn^{2+} phosphor for white-light-emitting diode, *Electrochem. Solid State Lett.* 8 (2005) H65–H67.
- [21] Y. Yonesaki, Q. Dong, N.S.B. Mohamad, A. Miura, T. Takei, J. Yamanaka, N. Kumada, N. Kinomura, Vitreous phase coating on glaserite-type alkaline earth silicate blue phosphor $\text{BaCa}_2\text{MgSi}_2\text{O}_8:\text{Eu}^{2+}$, *J. Alloys Compd.* 509 (2011) 8738–8741.
- [22] W.J. Yeo, C.J. Jeon, E.S. Kim, Dependence of thermal properties on crystallization behaviors of $(1-x)\text{MgSiO}_3-x\text{CaMgSi}_2\text{O}_6$ glass–ceramics, *Ceram. Int.*, in press, doi:10.1016/j.ceramint.2011.05.072.
- [23] E.P. Meagher, The atomic arrangement of pellyite: $\text{Ba}_2\text{Ca}(\text{Fe}, \text{Mg})_2\text{Si}_6\text{O}_{17}$, *Am. Mineral.* 61 (1976) 67–73.
- [24] R.D. Shannon, Revised effective ionic radii and systematic studies of interatomic distances in halides and chalcogenides, *Acta Crystallogr. A* 32 (1976) 751–767.
- [25] R.J. Xie, N. Hirotsuki, N. Kiumra, K. Sakuma, M. Mitomo, 2-Phosphor-converted white light-emitting diodes using oxynitride/nitride phosphors, *Appl. Phys. Lett.* 90 (2007) 191101–191103.